Altered Protein Function Caused by AMD-associated Variant rs704 Links Vitronectin to Disease Pathology

Fabiola Biasella,[1] Karolina Plössl,[1] Claudia Karl,[1] Bernhard H. F. Weber,[1,2] and Ulrike Friedrich[1]

[1]Institute of Human Genetics, University of Regensburg, Regensburg, Germany
[2]Institute of Clinical Human Genetics, University Hospital Regensburg, Regensburg, Germany

Correspondence: Ulrike Friedrich, Institute of Human Genetics, University of Regensburg, Building D3, Franz-Josef-Strauß-Allee 11, 93053 Regensburg, Germany; ulrike.friedrich@klinik.uni-regensburg.de.

Received: June 9, 2020
Accepted: November 7, 2020
Published: December 1, 2020

Citation: Biasella F, Plössl K, Karl C, Weber BHF, Friedrich U. Altered protein function caused by AMD-associated variant rs704 links vitronectin to disease pathology. *Invest Ophthalmol Vis Sci.* 2020;61(14):2. https://doi.org/10.1167/iovs.61.14.2

Purpose. Vitronectin, a cell adhesion and spreading factor, is suspected to play a role in the pathogenesis of age-related macular degeneration (AMD), as it is a major component of AMD-specific extracellular deposits (e.g., soft drusen, subretinal drusenoid deposits). The present study addressed the impact of AMD-associated non-synonymous variant rs704 in the vitronectin-encoding gene *VTN* on vitronectin functionality.

Methods. Effects of rs704 on vitronectin expression and processing were analyzed by semi-quantitative sequencing of *VTN* transcripts from retinal pigment epithelium (RPE) cells generated from human induced pluripotent stem cells (hiPSCs) and from human neural retina, as well as by western blot analyses on heterologously expressed vitronectin isoforms. Binding of vitronectin isoforms to retinal and endothelial cells was analyzed by western blot. Immunofluorescence staining followed extracellular matrix (ECM) deposition in cultured RPE cells heterologously expressing the vitronectin isoforms. Adhesion of fluorescently labeled RPE or endothelial cells in dependence of recombinant vitronectin or vitronectin-containing ECM was investigated fluorometrically or microscopically. Tube formation and migration assays addressed effects of vitronectin on angiogenesis-related processes.

Results. Variant rs704 affected expression, secretion, and processing but not oligomerization of vitronectin. Cell binding and influence on RPE-mediated ECM deposition differed between AMD-risk-associated and non-AMD-risk-associated protein isoforms. Finally, vitronectin affected adhesion and endothelial tube formation.

Conclusions. The AMD-risk-associated vitronectin isoform exhibits increased expression and altered functionality in cellular processes related to the sub-RPE aspects of AMD pathology. Although further research is required to address the subretinal disease aspects, this initial study supports an involvement of vitronectin in AMD pathogenesis.

Keywords: AMD, age-related macular degeneration, vitronectin, VTN, rs704

Age-related macular degeneration (AMD) is a complex degenerative disorder of the central retina for which individual genetic variants, as well as environmental and lifestyle factors, contribute to disease risk.[1,2] Currently, the molecular mechanisms of disease pathology are not fully understood, although irregularities in processes such as complement system regulation, extracellular matrix (ECM) remodeling, lipid metabolism, or vascular modifications are suspected in the disease pathogenesis.

Vitronectin, a cell adhesion and spreading factor,[3] was implicated in AMD in several studies reporting this protein as a major constituent of drusen[4–8] and of subretinal drusenoid deposits.[8–10] In addition, the cytoplasm of drusen-associated retinal pigment epithelial (RPE) cells from human donors was found to contain elevated amounts of vitronectin.[11] In vitro studies have shown an upregulation of vitronectin mRNA expression in human induced pluripotent stem cells (hiPSCs)–RPE cells derived from AMD patients,[12] as well as an upregulation of the vitronectin protein in complement-stimulated, immortalized RPE (ARPE-19) cells.[13]

Vitronectin is a secreted glycoprotein circulating in blood serum but has also been found to be deposited in the ECM of various tissues.[3] In the eye, vitronectin mRNA expression has been detected in the RPE, in photoreceptors, and in ganglion cells,[4,14] with higher expression levels in the neural retina compared to the RPE[15] (see also the eyeIntegration database, https://eyeintegration.nei.nih.gov). Conversely, extracellular labeling of vitronectin protein in the retina is limited primarily to Bruch's membrane and the retinal vasculature.[14] In particular, the inner collagenous layer of Bruch's membrane[16] and the basement membrane of endothelial cells[17] contain substantial amounts of vitronectin. The latter is important for endothelial cell migration and proliferation (reviewed in Dejana et al.[17]).

Two vitronectin isoforms are known; one is a single-chain molecule with a molecular weight of 75 kDa, and the other is a cleaved form consisting of two chains (65 and 10 kDa) connected via a disulfide bond.[18] Upon binding of specific ligands or interaction partners, unfolding of monomeric vitronectin leads to the formation of vitronectin multimers, stabilized by disulfide and non-covalent bonds.[19,20]

In the largest genome-wide association study known to date, Fritsche and colleagues[21] reported that a genetic variant, rs704, in the *VTN* gene was significantly associated with AMD. Specifically, rs704 is part of a 95% credible set comprised of 22 genetic variants at the *TMEM97–VTN* locus on chromosome 17.[21] Although lead variant rs11080055 is located in intron 1 of the *TMEM97* gene, it is still unclear which genetic variant at this locus may be functionally relevant. This will require a functional dissection of the effects of the risk-associated variants at this interval, although some investigations suggest that weighting sequence variants based on their annotation significantly increases the power to detect the causative variant of a locus.[22,23] Nevertheless, within the described 95% credible set, rs704 is the only missense and protein-altering variant.[21] Furthermore, due to its multifaceted function (reviewed in Leavesley et al.[3]), vitronectin could affect many processes involved in AMD pathogenesis, such as angiogenesis or extracellular matrix integrity (reviewed in Kleinman and Ambati[24] and Campochiaro[25]). Together with the already reported detection of vitronectin in AMD-related retinal tissues and deposits, this variant appears to be an excellent candidate for a targeted functional analysis within this credible set.

The single nucleotide polymorphism rs704, localized in exon 7 of the *VTN* gene, leads to an alteration from cytosine (C) to thymine (T) at nucleotide position 1199, resulting in an amino acid exchange from threonine to methionine at amino acid position 400. The replacement of threonine by methionine was previously shown to decrease the endogenous proteolytic cleavage of vitronectin and thus increase the presence of the single-chain vitronectin.[26]

Here, we compared the two vitronectin isoforms VTN_rs704:T (AMD-risk-associated) and VTN_rs704:C (non-AMD-risk-associated) in terms of protein expression, oligomerization, deposition, and functionality in AMD-related cellular processes. Our data reveal differences of the two isoforms in expression, cell binding, and their effects on ECM deposition and endothelial cell migration. Furthermore, both vitronectin isoforms affected cellular adhesion and endothelial formation of tubular-like structures. Together, our findings suggest a role for vitronectin in AMD pathogenesis.

Materials and Methods

Ethical Standards

In accordance with the tenets of the Declaration of Helsinki, postmortem human donor eyes were collected at the Ludwig Maximilian University of Munich and the University Hospital Cologne. Each study was approved by the corresponding local institutional review boards (application nos. MUC73416, Munich; 14-247, Cologne). All samples investigated in this study were approved for research use. Only clinically asymptomatic retinal samples with no sign of retinal pathology were included. Generation and analysis of hiPSC–RPE cells from human donor material have obtained approval of the ethics review board of the University of Regensburg, Germany (reference no. 12-101-0241 and amendment to 12-101-0241) and have been performed in accordance with the ethical standards laid down in the 1964 Declaration of Helsinki and its later amendments. Informed consent was given by each proband participating in the study.

Cell Culture

Y79 and WERI-Rb1 cells (American Type Culture Collection, Manassas, VA, USA) were cultivated in RPMI medium (Thermo Fisher Scientific, Waltham, MA, USA) with 10% fetal calf serum (FCS), as well as 100 U/mL penicillin/streptomycin. ARPE-19 cells (American Type Culture Collection) were maintained in Dulbecco's Modified Eagle Medium/Nutrient Mixture F-12 Ham medium (DMEM/HamsF12; Sigma-Aldrich, St. Louis, USA) containing 10% FCS and 100 U/mL penicillin/streptomycin. Human embryonic kidney cells (HEK293-EBNA; Invitrogen, Carlsbad, CA, USA) were maintained in DMEM high-glucose medium containing 10% FCS, 100 U/mL penicillin/streptomycin, and 500 µg/mL G418. Media and cell culture supplies were purchased from Life Technologies (Carlsbad, CA, USA). Human umbilical vein endothelial cells (HUVECs) were purchased from Life Technologies (Darmstadt, Germany) and cultured in EGMPlus Endothelial Cell Growth Media with EGMPlus SingleQuots supplements (Lonza Group, Ltd., Basel, Switzerland), but without gentamycin. HiPSC–RPE cells were generated as described in Nachtigal et al.[27] and Okita et al.[28] The hiPSC–RPE cells were cultured on 12-well or 24-well transwell filter inserts (0.4-µm pore size; Greiner Bio-One International, Kremsmünster, Austria) coated with Corning Matrigel Growth Factor Reduced (GFR) Basement Membrane Matrix (Corning, Corning, NY, USA) in Gibco KnockOut DMEM Medium supplied with 2-mM L-glutamine, 5% (v/v) KnockOut Serum Replacement, and 0.1-mM Gibco MEM Non-Essential Amino Acids Solution (all obtained from Life Technologies), as well as 5-µg/mL gentamycin, 0.1-mM β-mercaptoethanol, and 10-mM nicotinamide (Sigma-Aldrich). Differentiation was assessed as described previously,[29] specifically by investigating RPE-specific gene expression; localization of ZO-1, BEST-1, ATP1A1, and ATP1B1; and basal and apical secretion of vascular endothelial growth factor (VEGF), followed by enzyme-linked immunosorbent assay (R&D Systems, Abingdon, UK); see also Supplementary Figure S1. A stable high transepithelial resistance of $>150\ \Omega \times cm^2$ was obtained after 6 weeks of maturation ($233.3 \pm 53.2\ \Omega \times cm^2$). For propagation, cell lines were grown in a 37°C incubator with a 5% CO_2 environment and subcultured when reaching 90% confluency for HEK293, HUVECs, and ARPE-19 or a concentration of 4-5 $\times$ 10^5 cells/mL for Y79 and WERI-Rb1. Alterations of these cultivation conditions were used for functional assays and are described in the following subsections.

DNA and RNA Analysis

RNA from hiPSC–RPE or human neural retina was isolated using the PureLink RNA Micro Kit (Invitrogen), according to the manufacturer's protocols. One microgram of total RNA was transcribed into cDNA using RevertAid M-MuLV Reverse Transcriptase (Fermentas, St. Leon-Rot, Germany) and poly(dT) primers according to the manufacturer's instructions. Semi-quantitative RT-PCR was performed as described in Friedrich et al.[30] with primers given in Supplementary Table S1. DNA isolation and PCR with genomic DNA were performed as described in Friedrich et al.[31] Primers for PCR with genomic DNA are shown in Supplementary Table S1. Sequencing of the RT-PCR products and the genomic PCR products was performed as described in Friedrich et al.[31] with the primers shown in Supplementary Table S1.

Antibodies

Applied antibodies, their origin, and dilutions for western blot or immunocytochemical analyses are given in Supplementary Table S2.

Expression Cloning

After genotyping of ARPE-19 cells that were heterozygous for rs704, the coding sequences for VTN_rs704:C and VTN_rs704:T were amplified from cDNA of ARPE-19 cells. The fragments were cloned into the BamHI/XhoI site of the pEXPR-IBA103 vector (IBA Life Sciences, Göttingen, Germany) fusing them to a Twin-Strep-tag (IBA Life Sciences). Generated vectors allowing expression of Strep-tagged vitronectin were named pEXPR-IBA103-VTN_rs704:C and pEXPR-IBA103-VTN_rs704:T. For heterologous expression of untagged protein, *VTN*_rs704:C and *VTN*_rs704:T were cloned into the NotI/XhoI site of the pcDNA3.1 vector (Invitrogen). Generated vectors were named pcDNA3.1-VTN_rs704:C and pcDNA3.1-VTN_rs704:T. To generate a green fluorescent protein (GFP) expression vector, the GFP coding sequence was cloned into the BamHI/NotI site of pcDNA3.1 (the resulting vector was named pcDNA3.1-GFP). Primer sequences and applied polymerase are given in Supplementary Table S1.

Heterologous Expression and Purification of Recombinant Vitronectin Isoforms

To explore the effects of rs704 on vitronectin expression and secretion, HEK293 and ARPE-19 cells were co-transfected with pcDNA3.1-GFP and pcDNA3.1, pcDNA3.1-VTN_rs704:C, or pcDNA3.1-VTN_rs704:T, using TransIT-LT1 Transfection Reagent (Mirus Bio, Madison, WI, USA) for HEK293 or Lipofectamine 3000 Transfection Reagent (Thermo Fisher Scientific) for ARPE-19, according to the manufacturer's instructions. Vitronectin expression was investigated in cell pellets and supernatants via sodium dodecyl sulfate–polyacrylamide gel electrophoresis (SDS-PAGE) and western blot analysis. The applied antibody against vitronectin (see Supplementary Table S2) is a monoclonal antibody generated against human plasma-derived vitronectin. It detects the full length (75 kDa) isoform, as well as the 65 kDa subfragment, but not the 10-kDa subfragment of the cleaved isoform (see also Supplementary Fig. S2).

To isolate and purify vitronectin isoforms, pEXPR-IBA103-VTN_rs704:C or pEXPR-IBA103-VTN_rs704:T were transfected into HEK293 by the calcium phosphate method as described previously.[32] Seven hours after transfection, the culture medium was replaced by FCS-free DMEM high-glucose medium containing 100 U/mL penicillin/streptomycin and 500 µg/mL G418, and cells were cultured for 72 hours. Strep-tagged VTN_rs704:C and VTN_rs704:T were purified with the Twin-Strep-tag purification kit from the supernatant of transfected HEK293 cells according to the manufacturer's protocol. Concentrations of purified proteins were determined using the Bio-Rad DC protein assay kit (Bio-Rad Laboratories, Hercules, CA, USA), as well comparative western blot analysis with recombinant vitronectin protein (10424-H08H; Sino Biological, Inc., Beijing, China). As a control, HEK293 cells were transfected with empty pEXPR-IBA103 expression vector, and the cultivation medium of these cells was subjected to purification procedures identical to that for cells transfected with vitronectin expression vectors. Enrichment and purification were controlled via silver staining, Coomassie Blue staining, and western blot analysis (see Supplementary Fig. S3).

SDS-PAGE and Western Blot Analysis

SDS-PAGE and western blot analysis were performed as described previously.[30,33,34] Non-reducing conditions were established by omitting the reducing agent β-mercaptoethanol from Lämmli buffer[35] in gels containing 7% acrylamide. Densitometry was done with Image Studio software (LI-COR Biosciences, Lincoln, NE, USA).

Blue Native PAGE

All supplies (gels, buffers, standard) for Blue native PAGE were purchased from the Invitrogen NativePAGE range (Thermo Fisher Scientific). Blue native gel electrophoresis was performed according to the manufacturer's instructions. For western blot analyses, the NuPAGE Transfer Buffer (Thermo Fisher Scientific) system for wet blotting was used according to the manufacturer's instructions.

Binding of Vitronectin Isoforms to Cells

Vitronectin binding to cell lines (ARPE-19, hiPSC–RPE, porcine RPE, Y79, and HUVECs) was assessed as described previously,[30,36] with the following modifications. Cells grown to confluency in one 10-cm plate (ARPE-19), six 12-well transwell filters inserts (hiPSC–RPE), or one T25 flask (HUVECs), as well as to maximal cell concentration in two T25 flasks (Y79), were suspended as combined samples in 600 µL Dulbecco's phosphate-buffered saline (DPBS; Sigma-Aldrich). Porcine RPE cells were dissected from fresh eyes obtained from a local slaughterhouse as described previously.[37] Cells obtained from one eye were resuspended in 600 µL DPBS. Then, 200 µL of the cell suspensions were incubated with 1 mL VTN_rs704:C-containing medium, VTN_rs704:T-containing medium, or control medium (from supernatant of transfected HEK293 cells) for 60 minutes, with subsequent washing steps as described previously.[30,36]

Production of ARPE-19 Cell-Derived ECM Containing Overexpressed Vitronectin Isoforms

To generate cell-derived ECM, ARPE-19 cells were co-transfected with pcDNA3.1-GFP and pcDNA3.1, pcDNA3.1_VTN_rs704:C, or pcDNA3.1_VTN_rs704:T using Lipofectamine 3000 Transfection Reagent (Thermo Fisher Scientific) according to the manufacturer's instructions. After 24 hours, GFP fluorescence was microscopically assessed as a marker for transfection efficiency. Transfected ARPE-19 cells were enzymatically dissociated from the cell culture plate with Gibco Trypsin–EDTA (Thermo Fisher Scientific) and seeded onto 12- or 24-well transwell filter inserts (0.4-µm pore size; Greiner Bio-One), with 4×10^5 cells or 2×10^5 cells per transwell filter insert in DMEM/HamsF12 containing 10% FCS and 100 U/mL penicillin/streptomycin. After 24 hours, the medium was changed to FCS-free medium containing 100 U/mL penicillin/streptomycin, 200 µg/mL dextran sulfate (Carl Roth GmbH, Karlsruhe, Germany), and 30 µg/mL ascorbic acid (Cayman

Chemical, Ann Arbor, MI, USA), as described in McLenachan et al.[38] Confluent ARPE-19 monolayers were cultured in this medium for 4 weeks with media changes three times per week. Transwell filter inserts were then decellularized by incubating them with 0.5% Triton X-100 and 20-mM NH_4OH in DPBS for 5 minutes at 37°C, as described in Fernandez-Godino et al.[39] Immunolabeling was performed as described in Friedrich et al.[30] and Schmid et al.[40] using a quarter of a 12-well transwell filter insert for each staining. Pictures were taken with a confocal laser scanning microscope (FV3000 Fluoview; Olympus Life Sciences, Hamburg, Germany). Signal intensity and average cluster size were measured using ImageJ (National Institutes of Health, Bethesda, MD, USA).

Adhesion Assay with Purified Recombinant Vitronectin Isoforms

HiPSC–RPE cells were enzymatically dissociated from 12-well transwell filter inserts with Gibco TrypLE Select (Thermo Fisher Scientific) for 40 minutes at 37°C. Subsequently, cells from a single filter were resuspended in 600 µL medium (deprived of KnockOut Serum Replacement), after which 100 µL of the cell suspension was mixed with 1.5 µg/mL of purified recombinant vitronectin isoforms (VTN_rs704:C or VTN_rs704:T) or equal volumes of control eluates and then transferred onto a 96-well plate. After 24 hours of incubation at 37°C, the medium was removed, and cells were incubated with Hoechst 33342 (1:1000 diluted in DPBS) for 10 minutes at room temperature. After staining, cells were washed three times for 5 minutes each with DPBS. Fluorescence images of adherent cells were taken with a Nikon Eclipse microscope (TE-2000-U; Nikon, Tokyo, Japan). Cell attachment was quantified by fluorescence intensity measurement (excitation/emissions, 360/490 nm) using a Spark multimode microplate reader (Tecan Group AG, Männedorf, Switzerland).

The adhesion assay with primary porcine RPE cells was performed similarly, with minor modifications. Porcine RPE cells were dissected from fresh eyes obtained from a local slaughterhouse as described previously.[37] Cells obtained from one eye were resuspended in 600 µL medium (deprived of KnockOut Serum Replacement), and 100 µL of the cell suspension was applied to the adhesion assay with an incubation time of 18 hours. Due to the strong pigmentation, fluorescent staining with Hoechst 33342 was omitted. Images from each 96-well plate were taken at 4× magnification with a Nikon Eclipse microscope, and RPE cells were counted using ImageJ.

The HUVEC adhesion assay was performed likewise, with minor modifications. Briefly, cells from a T25 cell culture flask were enzymatically dissociated with 1 mL of Trypsin–EDTA for 1 minute at room temperature and resuspended in 1.2 mL FCS-free cultivation medium. Then, 100 µL of the cell suspension was applied to the adhesion assay. Incubation time was 20 minutes.

Adhesion Assay on ARPE-19-Derived ECM

A volume of 200 µL hiPSC–RPE, 250 µL porcine RPE, or 200 µL HUVEC cell suspension (prepared as described in the preceding paragraph) was transferred onto a 24-well transwell filter insert coated with ARPE-19-derived ECM. After 40 minutes (hiPSC–RPE or porcine RPE cells) or 20 minutes (HUVECs), the culture medium was removed. The hiPSC–RPE cells or HUVECs were incubated with Hoechst 33342 as described above. Images from each transwell filter insert were taken at 4× magnification with a Nikon Eclipse microscope. Cells were counted using ImageJ.

HUVEC Tube Formation Assay

Endothelial tube formation in response to vitronectin exposure was examined in vitro with HUVECs as described in Ponce[41] with the following modifications: First, 8.5×10^3 HUVECs/well were seeded onto a 96-well plate coated with 37.5 µL Geltrex LDEV-Free Reduced Growth Factor Basement Membrane Matrix (Thermo Fisher Scientific). Cells were then cultured in 100 µL EGMPlus Endothelial Cell Growth Media containing 1/3 EGMPlus SingleQuots supplements, 50 ng/mL VEGF (PeproTech, Hamburg, Germany), and 5 µg/mL purified recombinant vitronectin (VTN_rs704:C or VTN_rs704:T) or equal volumes of control eluate. Three to five simultaneous tests per each treatment were included in one independent replicate. After 16 hours, images from each well were captured at 4× magnification with a Nikon Eclipse microscope. Cumulative tube length was quantified using the Angiogenesis Analyzer in ImageJ as described previously.[42]

HUVEC Migration Assay

HUVEC migration was determined using the scratch-wound assay, as described in Liang et al.[43] with the following modifications. HUVECs were seeded on a 96-well plate and incubated in EGMPlus Endothelial Cell Growth Media with EGMPlus SingleQuots supplements. After 24 hours, confluent cell monolayers were scratched using a WoundMaker (Essen BioScience, Ann Arbor, MI, USA). Cell debris was removed by washing with DPBS, and injured monolayers were incubated in EGMPlus Endothelial Cell Growth Media with EGMPlus SingleQuots supplements but without FCS, containing 50 ng/mL VEGF, and 20 µg/mL of purified recombinant vitronectin (VTN_rs704:C or VTN_rs704:T) or equal volumes of control eluate. Four to seven simultaneous tests per treatment were included in one independent replicate. After 0 and 14 hours, images from each well were captured at 4× magnification with a Nikon Eclipse microscope. Scratch areas were determined using ImageJ, and migration ability was defined as the percentage area closed after 14 hours of incubation.

Statistical Analyses

Statistical analyses were performed with the XLSTAT add-in software. The Shapiro–Wilk normality test was applied to assess normality of the data. Data following a Gaussian distribution were analyzed using Student's *t*-test (two experimental groups) or ANOVA test with Tukey's multiple comparison test (more than two experimental groups). Data not following a Gaussian distribution were analyzed with the Mann–Whitney *U* test (two experimental groups) or Kruskal–Wallis test with post ad hoc Dunn's multiple comparison test and Bonferroni correction (more than two experimental groups).

Results

Endogenous Vitronectin Expression in Retinal and Non-Retinal Cell Lines

Searching for in vitro model systems applicable to analyzing an influence of rs704 on vitronectin functionality, we tested endogenous vitronectin expression in different retinal and non-retinal cells frequently used as model systems to investigate AMD-associated molecular pathomechanisms or functionality of retinal disease-related proteins.[12,34,44] These included human RPE cell lines ARPE-19 and hiPSC–RPE, human retinoblastoma cell lines Y79 and WERI-Rb1, endothelial cell line HUVEC, and HEK293 cells.

Endogenous vitronectin mRNA expression, assessed using semi-quantitative RT-PCR (Fig. 1A), was only detected in the two retinoblastoma-derived cell lines Y79 and WERI-Rb1 and, to a much weaker extent, in the two RPE cell lines ARPE-19 and hiPSC–RPE. Western blot analysis, however, failed to detect vitronectin protein in any of the cell lines tested, even after multiple attempts to increase sensitivity (Fig. 1B).

In the human retina, *VTN* is expressed in RPE and neural retina[4,14,15] (see also the eyeIntegration database, https://eyeintegration.nei.nih.gov). An effect of rs704 on mRNA expression in these tissues was measured by a semi-quantitative sequencing approach on hiPSC–RPE cells and neural retinal samples derived from different donors, which were heterozygous for rs704 (identified via genomic sequencing; see Supplementary Fig. S2). A dilution series with different concentrations of the vitronectin mRNA variants (*VTN*_rs704:C and *VTN*_rs704:T) showed that the rs704 polymorphism of the *VTN* gene is resolvable as a heterozygous peak in the sequence chromatogram up to the highest dilution of 1:5. Differences in *VTN*_rs704:C and *VTN*_rs704:T concentrations are traceable at changes in the electropherogram peaks of the T and the C allele at the rs704 position from a twofold increase in one of the two variants (Fig. 1C). Analyzing vitronectin mRNA expression in the heterozygous hiPSC–RPE cell lines and neural retinal samples (Fig. 1D) revealed similar electropherogram peaks for the T and the C allele at the rs704 position (Fig. 1D), suggesting similar levels of *VTN*_rs704:C and *VTN*_rs704:T transcripts and thus no significant effect of rs704 on vitronectin mRNA expression in these samples.

Effect of rs704 on Vitronectin Protein Expression, Processing, and Oligomerization

Next, an effect of rs704 on vitronectin protein expression and secretion was analyzed. To this end, HEK293 and ARPE-19 cells were transfected with expression vectors for the two vitronectin isoforms: the non-AMD-risk-associated isoform VTN_rs704:C and the AMD-risk-associated isoform VTN_rs704:T. Western blot analysis followed by densitometric evaluation (see Supplementary Fig. S2) determined vitronectin processing and vitronectin protein expression in cells and supernatants at two different time points (48 hours and 72 hours after transfection) (Fig. 2A). Heterologous expression of vitronectin isoforms in HEK293 cells revealed a statistically significant increase in intracellular amounts of AMD-risk-associated VTN_rs704:T relative to the non-AMD-risk-associated VTN_rs704:C (48 hours, 3.99 ± 2.88-fold increase; 72 hours, 5.66 ± 1.91-fold increase; $P < 0.05$ for both time points). Similarly, an

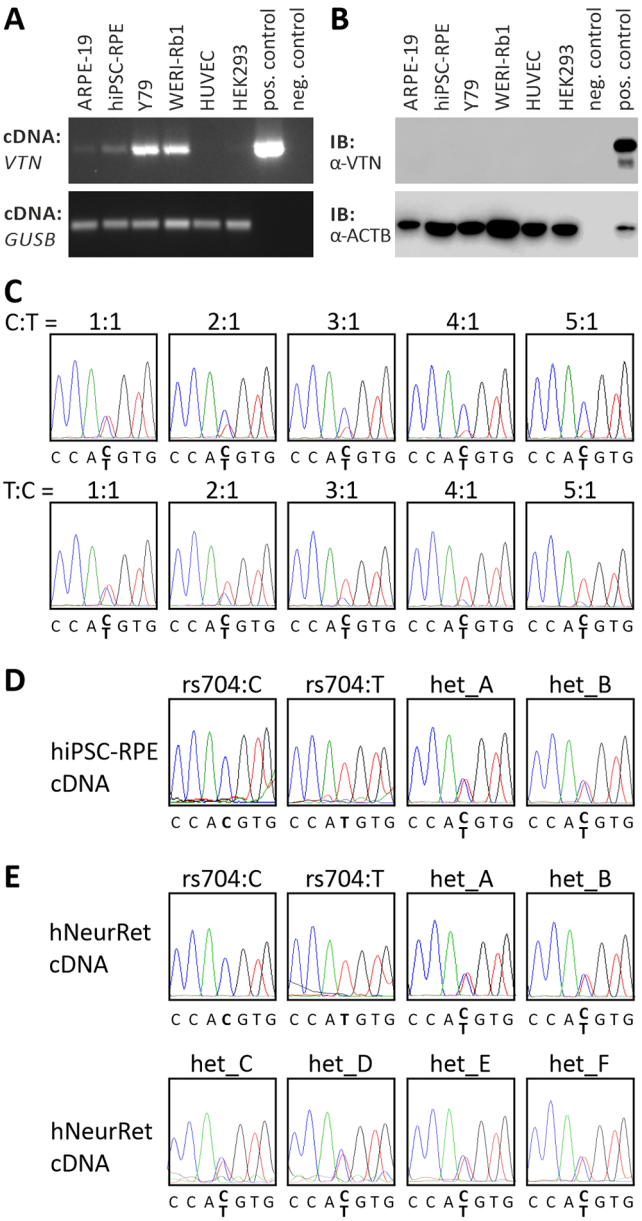

Figure 1. Endogenous vitronectin expression in retinal and non-retinal cell lines. (**A**) RT-PCR analysis of *VTN* gene expression in ARPE-19, hiPSC–RPE, Y79, WERI-Rb1, HUVEC, and HEK293 cells. Expression vectors containing cDNA of non-AMD-risk-associated *VTN* served as positive control; no template was added to the negative control. *GUSB* gene expression was assessed as control for RNA integrity. (**B**) Western blot analysis of vitronectin protein expression in ARPE-19, hiPSC–RPE, Y79, WERI-Rb1, HUVEC, and HEK293 cells. HEK293 cells transfected with expression vectors for VTN_rs704:C served as positive control. Cell lysates were subjected to western blot analyses using antibodies against vitronectin. The ACTB immunoblot was performed as loading control. (**C**) Titration series with recombinant *VTN* cDNA isoforms derived from the non-risk (rs704:C) or the risk (rs704:T) haplotype (ratio of C:T allele given in the figure). Isoforms were determined by sequence analysis. *VTN*_rs704:C and *VTN*_rs704:T transcription in hiPSC–RPE cells (**D**) or human retinal tissues (**E**) of different donors was analyzed by semi-quantitative sequencing of allele-specific transcripts. Non-AMD-risk-associated and AMD-risk-associated alleles at the vitronectin gene locus were determined by genomic sequencing of variant rs704 (see Supplementary Fig. S4). Expression of the non-AMD-risk-associated and AMD-risk-associated *VTN* mRNA isoforms was investigated by cDNA sequencing of variant rs704.

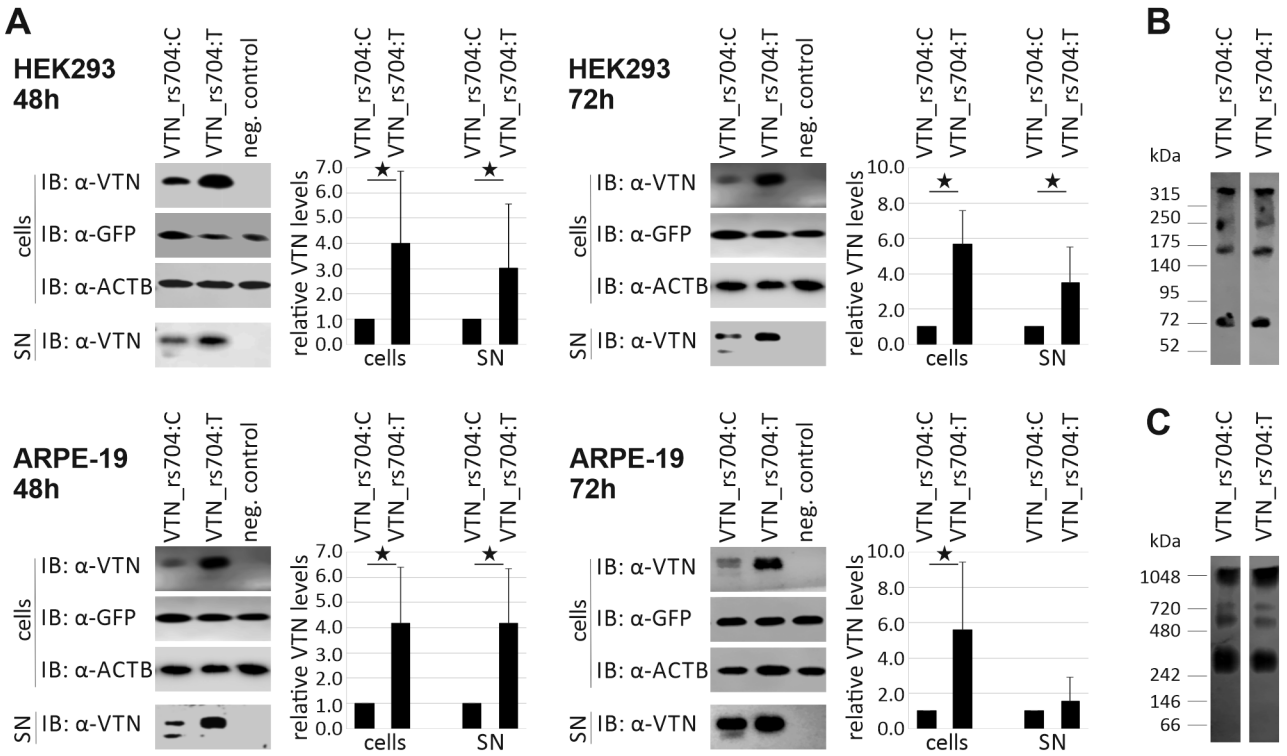

Figure 2. Effect of rs704 on vitronectin protein expression, processing, and oligomerization. (**A**) Western blot analysis of VTN_rs704:C or VTN_rs704:T protein expression after heterologous expression. HEK293 and ARPE-19 cells were transfected with expression vectors for VTN_rs704:C or VTN_rs704:T or with an empty expression vector (pcDNA3.1). Co-transfection with a GFP expression vector was performed as control. Forty-eight and 72 hours after transfection, cell pellets and supernatants (SNs) of transfected cells were subjected to western blot analysis with antibodies against vitronectin and GFP. The ACTB immunoblot served as control. After densitometric quantification, vitronectin signals from cell pellets and supernatants were normalized against GFP. Data represent the mean ± SD of four biological replicates, calibrated against VTN_rs704:C. Asterisks indicate statistically significant differences ($^{*}P < 0.05$, Mann–Whitney *U* test). (**B**) Non-reducing SDS-PAGE and (**C**) Blue native PAGE with purified recombinant vitronectin isoforms, followed by western blot analysis against vitronectin.

increase of VTN_rs704:T protein relative to VTN_rs704:C was evident in the supernatant of the transfected HEK293 cells (48 hours, 3.03 ± 2.52-fold increase; 72 hours, 3.47 ± 2.05-fold increase; $P < 0.05$ for both time points). Comparable results were obtained after heterologous expression of vitronectin isoforms in ARPE-19. Compared to VTN_rs704:C, the AMD-risk-associated VTN_rs704:T showed a statistically significant increase in intracellular protein level (48 hours, 4.19 ± 2.20-fold increase; 72 hours, 5.60 ± 3.83-fold increase; $P < 0.05$ for both time points), as well as in the supernatant (48 hours, 4.17 ± 2.16-fold increase, $P < 0.05$; 72 hours, 1.55 ± 1.36-fold increase, $P > 0.05$).

The immunoblots of the supernatants demonstrated that VTN_rs704:T was less susceptible to endogenous cleavage, resulting in higher amounts of uncleaved, single-chain vitronectin and lower amounts of cleaved vitronectin, compared to VTN_rs704:C (Fig. 2A).

We further investigated the impact of rs704 on vitronectin oligomerization, which is thought to play an important role in cell adhesion, ECM organization, or the formation of extracellular deposits.[19,45,46] Vitronectin oligomerization is reported to be stabilized by disulfide bonds and non-covalent interactions.[19] To follow the formation of oligomers stabilized by disulfide bonds, non-reducing SDS-PAGE (Fig. 2B) was performed as described previously.[47,48] Oligomerization stabilized by non-covalent interactions was addressed via Blue native PAGE (Fig. 2C) as described previously.[49] Despite the effect of rs704 on endogenous proteolytic cleavage of the two vitronectin isoforms (Fig. 2A), rs704 did not affect oligomerization of the two vitronectin isoforms: non-reducing SDS-PAGE and Blue native PAGE both demonstrated similar oligomerization patterns for VTN_rs704:C and VTN_rs704:T (Figs. 2B, 2C).

Binding Capacity of Vitronectin Isoforms to Different Retinal and Non-Retinal Cell Lines

Under physiological conditions, soluble vitronectin binds to various cell surfaces.[50] We therefore investigated an influence of the rs704-associated amino acid exchange on the capacity of the two vitronectin isoforms to bind to retinal and endothelial cells (Fig. 3). All tested cell lines (ARPE-19, hiPSC–RPE, porcine RPE, HUVEC, and Y79) bound both vitronectin isoforms (VTN_rs704:C and VTN_rs704:T). However, a striking difference was evident in binding efficiency. Compared to the non-AMD-risk-associated VTN_rs704:C, the AMD-risk-associated VTN_rs704:T protein revealed a strongly decreased binding capacity to all cell lines tested (reduction to 21.3% ± 19.4% at ARPE-19, 34.8% ± 37.0% at hiPSC–RPE, 10.2% ± 6.7% at porcine RPE,

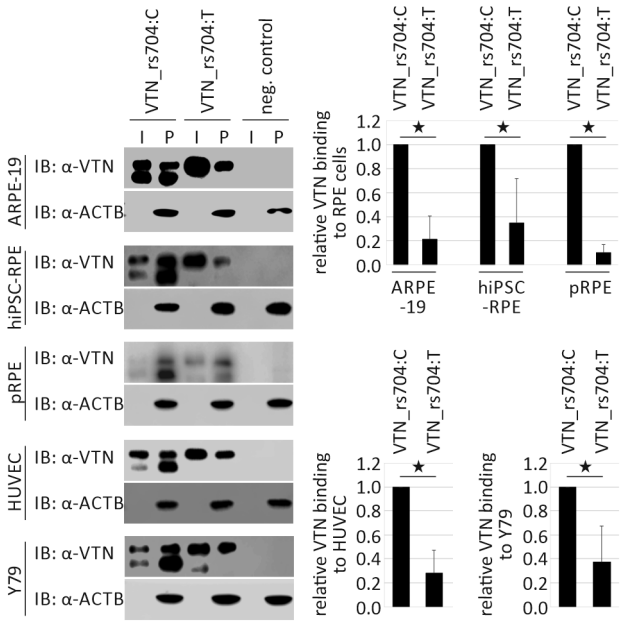

Figure 3. Binding capacity of vitronectin isoforms to different retinal and non-retinal cell lines. ARPE-19, hiPSC–RPE, porcine RPE (pRPE), HUVEC, and Y79 cells were incubated for 60 minutes with vitronectin-containing input (I, supernatants of HEK293 cells transfected with expression vectors for VTN_rs704:C and VTN_rs704:T, adjusted to obtain comparable concentrations of the vitronectin isoforms) or control input. Cells were then centrifuged and intensively washed. Vitronectin binding was assessed by subjecting cell pellets (P) to western blot analysis with antibodies against vitronectin. The ACTB immunoblot was performed as loading control. After densitometric quantification, vitronectin signals were normalized against ACTB and vitronectin in the input. Data represent the mean ± SD of four (hiPSC–RPE and pRPE), five (ARPE-19 and HUVECs), or six (Y79) biological replicates, calibrated against VTN_rs704:C. Asterisks indicate statistically significant differences ($^{*}P < 0.05$, Mann–Whitney *U* test).

27.9% ± 19.2% at HUVEC, and 37.1% ± 30.3% for Y79 cells; $P < 0.05$ for all cell lines).

Effect of rs704 on AMD-Associated Processes

In the retina, extracellular vitronectin protein was mainly detected in sub-RPE regions, namely in Bruch's membrane and the retinal vasculature.[14] As vitronectin is a known cell adhesion and spreading factor contributing to ECM organization (reviewed in Leavesley et al.[3]), we analyzed the role of the vitronectin isoforms in ECM deposition, RPE and endothelial adhesion, and spreading of endothelial cells, all processes associated with AMD pathology[51] (reviewed in Kleinman and Ambati[24] and Campochiaro[25]).

Effect of Vitronectin on Extracellular Microenvironment

To assess effects of vitronectin isoforms on ECM organization, we examined ECM deposition by ARPE-19 cells that were transfected with expression vectors for the two vitronectin isoforms, VTN_rs704:C or VTN_rs704:T, as described previously.[38,39]

After 4 weeks, ARPE-19 cells heterologously expressing vitronectin exhibited large extracellular vitronectin aggregates extending along the produced ECMs (Fig. 4A). Quantification revealed a 2.82 ± 1.89-fold increase in vitronectin signal intensity and a 1.99 ± 1.04-fold increase in vitronectin cluster size in the ECMs containing the AMD-risk-associated isoform VTN_rs704:T compared to ECMs containing non-AMD-risk-associated isoform VTN_rs704:C ($P < 0.05$) (Fig. 4B). Laminin staining reflected disorganized fibers and aggregates in all ECMs (Fig. 4A). The overall amount of laminin (Fig. 4B) and its assembly (Fig. 4C) were not affected by heterologous expression of vitronectin.

Fibronectin appeared as densely packed aggregates in ECMs of non-vitronectin expressing cells. In ECMs containing vitronectin, these aggregates extended and formed fibers (Fig. 4A), with an increase in total fibronectin signal intensity (VTN_rs704:C, 1.50 ± 0.64; VTN_rs704:T, 1.95 ± 1.15, compared to control) (Fig. 4B). The increase in fibronectin cluster size was 1.44 ± 0.64 for VTN_rs704:C and 2.50 ± 1.12 for VTN_rs704:T. The AMD-risk-associated VTN_rs704:T protein exerted a stronger effect on fibronectin levels and cluster sizes than VTN_rs704:C ($P < 0.05$ between VTN_rs704:T and control) (Figs. 4B, 4C).

Elastin revealed a similar appearance than fibronectin staining (Fig. 4A), although the increase in signal intensity was not as pronounced (VTN_rs704:C, 1.08 ± 0.05; VTN_rs704:T, 1.12 ± 0.06, compared to control; $P < 0.05$ between VTN_rs704:T and control) (Fig. 4B). Both vitronectin isoforms had a similar effect on elastin cluster size (increase to 1.62 ± 0.45 for VTN_rs704:C and 1.51 ± 0.34 for VTN_rs704:T compared with control; $P < 0.05$ between both vitronectin isoforms and control) (Fig. 4C).

In the ECMs of non-vitronectin expressing cells, collagen VI was evenly distributed along the ECM without prominent cluster or fiber formation. In vitronectin-containing ECMs, we observed a notable aggregation of collagen VI (Fig. 4A, shown in the merged picture of vitronectin and collagen VI staining). Although collagen VI staining failed to show a statistically significant increase in total signal intensity (Fig. 4B), vitronectin expression was associated with an increase in collagen VI cluster size. Again, AMD-risk-associated VTN_rs704:T exerted a stronger effect than non-AMD-risk-associated VTN_rs704:C (1.45 ± 0.42 for VTN_rs704:C and 1.81 ± 0.35 for VTN_rs704:T compared to control; $P < 0.05$ between VTN_rs704:T and control) (Fig. 4C).

Effect of Vitronectin on RPE and Endothelial Cell Adhesion

An effect of the vitronectin isoforms on RPE adhesion was analyzed by testing adherence of suspended hiPSC–RPE cells to the cell culture dish surface in the presence of purified recombinant VTN_rs704:C, VTN_rs704:T, or control eluate. After washing, adherent cells were labeled, and fluorescence intensity was measured fluorometrically (Fig. 5A). RPE adhesion increased to 4.24 ± 0.99 in VTN_rs704:C and to 3.78 ± 0.86 in VTN_rs704:T treated samples compared with control ($P < 0.05$ between vitronectin treated samples and control). Vitronectin-dependent RPE adhesion was also investigated using primary RPE cells, freshly isolated from pig eyes. Due to the strong pigmentation, adhesion was not followed fluorometrically, but microscopically. Again, the presence of recombinant vitronectin increased porcine RPE cell adhesion compared with control treatment (1.92 ± 0.53 for VTN_rs704C and 1.96 ± 0.83 for VTN_rs704:T; $P <$

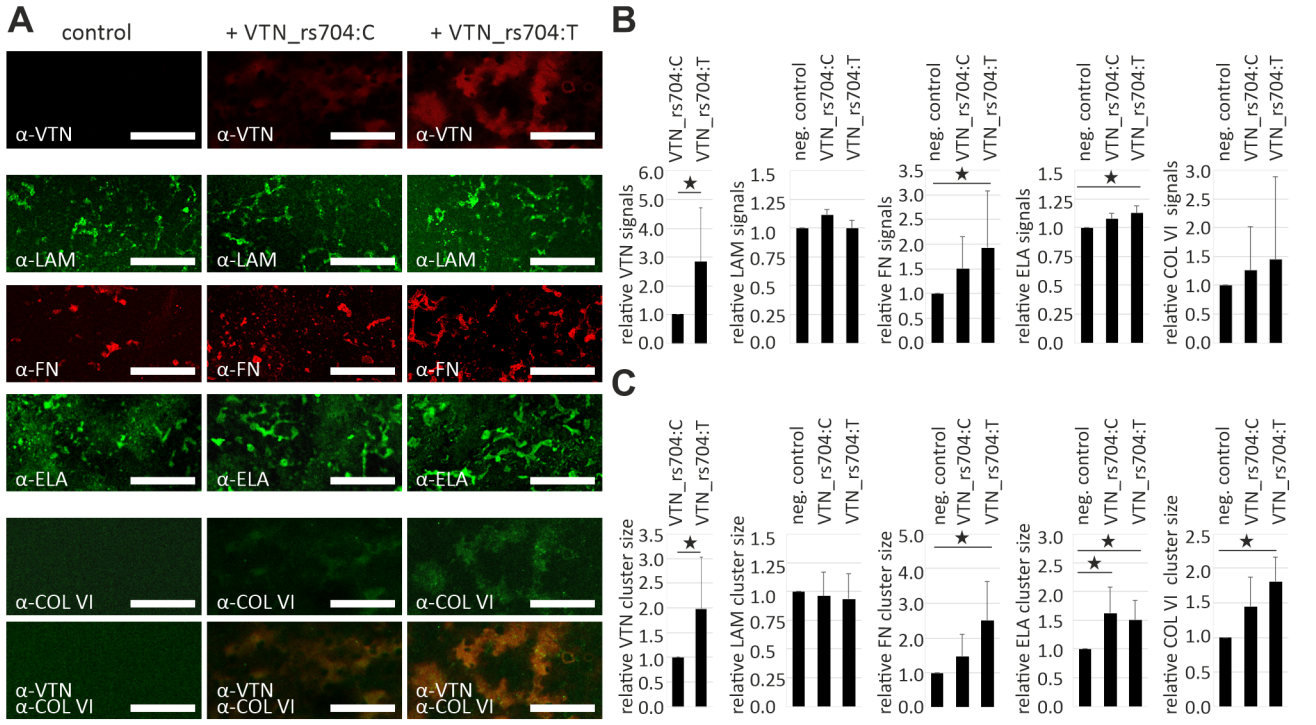

Figure 4. Effect of vitronectin isoforms on ECM deposition by ARPE-19 cells. (**A**) ARPE-19 cells transfected with expression vectors for VTN_rs704:C or VTN_rs704:T or with an empty expression vector (pcDNA3.1) were incubated for 4 weeks on transwell filter inserts. After 4 weeks, the inserts were decellularized and subjected to immunostaining with antibodies against vitronectin (α-VTN), laminin (α-LAM), fibronectin (α-FN), elastin (α-ELA), or collagen VI (α-COL VI). Confocal microscopy images were taken at 10× magnification. *Scale bars*: 100 µm. (**B**) Fluorescence intensity and (**C**) average cluster size were measured using ImageJ. Data represent the mean ± SD of eight (vitronectin), five (laminin, fibronectin, and elastin), or six (collagen VI), independent replicates, calibrated against the control. Asterisks indicate statistically significant differences ($^{*}P < 0.05$, Kruskal–Wallis test, followed by Dunn's multiple comparison test with Bonferroni correction).

0.05 between vitronectin treated samples and control). Interestingly, opposite results were obtained with endothelial HUVECs (Fig. 5B). The presence of recombinant vitronectin slightly decreased HUVEC adhesion and thus fluorescence intensity to 0.90 ± 0.05 for VTN_rs704:C and 0.83 ± 0.09 for VTN_rs704:T ($P < 0.05$ between VTN_rs704:T and control).

In an alternative approach, we tested RPE and endothelial cell adhesion to vitronectin-containing ECM deposited by ARPE-19. ECM containing recombinant vitronectin facilitated increased adherence of hiPSC–RPE cells (1.79 ± 0.41 for VTN_rs704C and 1.84 ± 0.25 for VTN_rs704:T; $P < 0.05$ between control and vitronectin-containing ECMs), porcine RPE cells (2.92 ± 1.71 for VTN_rs704C and 1.73 ± 0.42 for VTN_rs704:T; $P < 0.05$ between VTN_rs704:C-containing ECM and control), as well as of HUVECs (1.52 ± 0.36 for VTN_rs704C and 1.59 ± 0.56 for VTN_rs704:T; $P < 0.05$ between control and vitronectin-containing ECMs).

Effect of Vitronectin on Angiogenesis-Related Processes

Finally, we assessed effects of vitronectin isoforms on angiogenesis by testing HUVEC migration and the ability of HUVEC to form three-dimensional capillary-like tubular structures. The presence of recombinant purified VTN_rs704:C but not VTN_rs704:T slightly reduced HUVEC migration (VTN_rs704:C, 93.3% ± 5.0% compared to control; $P < 0.05$ between VTN_rs704:C and control, as well as between VTN_rs704:C and VTN_rs704:T) (Fig. 6A, Supplementary Fig. S5). Both vitronectin isoforms decreased tubular structure formation by HUVECs (reduction to 78.8% ± 27.2% by VTN_rs704:C and 85.2% ± 11.9% by VTN_rs704:T compared to control; $P < 0.05$ between control and both vitronectin isoforms) (Fig. 6B).

Discussion

The present study investigates the influence of AMD-associated genetic non-synonymous *VTN* variant rs704 on the functionality of the resulting vitronectin protein isoforms. We provide evidence that rs704 significantly alters expression, secretion, and processing of the vitronectin protein. In addition, rs704 affects the ability of vitronectin to bind to retinal and endothelial cells. Interestingly, the AMD-risk-associated and non-AMD-risk-associated vitronectin isoforms reveal differential effects on ECM production by ARPE-19 cells, specifically on deposition and clustering of ECM constituents such as fibronectin, elastin, and collagen VI. Vitronectin also affects RPE and endothelial cell adhesion, as well as tubular-like structure formation by endothelial cells. In consequence, our data suggest a close functional correlation between rs704 and vitronectin in AMD pathogenesis.

The cDNA analysis of hiPSC–RPE cells and human retinal tissues heterozygous for rs704 revealed no effect of rs704 on the transcriptional activity of *VTN*. This is consistent with data provided by the Genome-Tissue Expres-

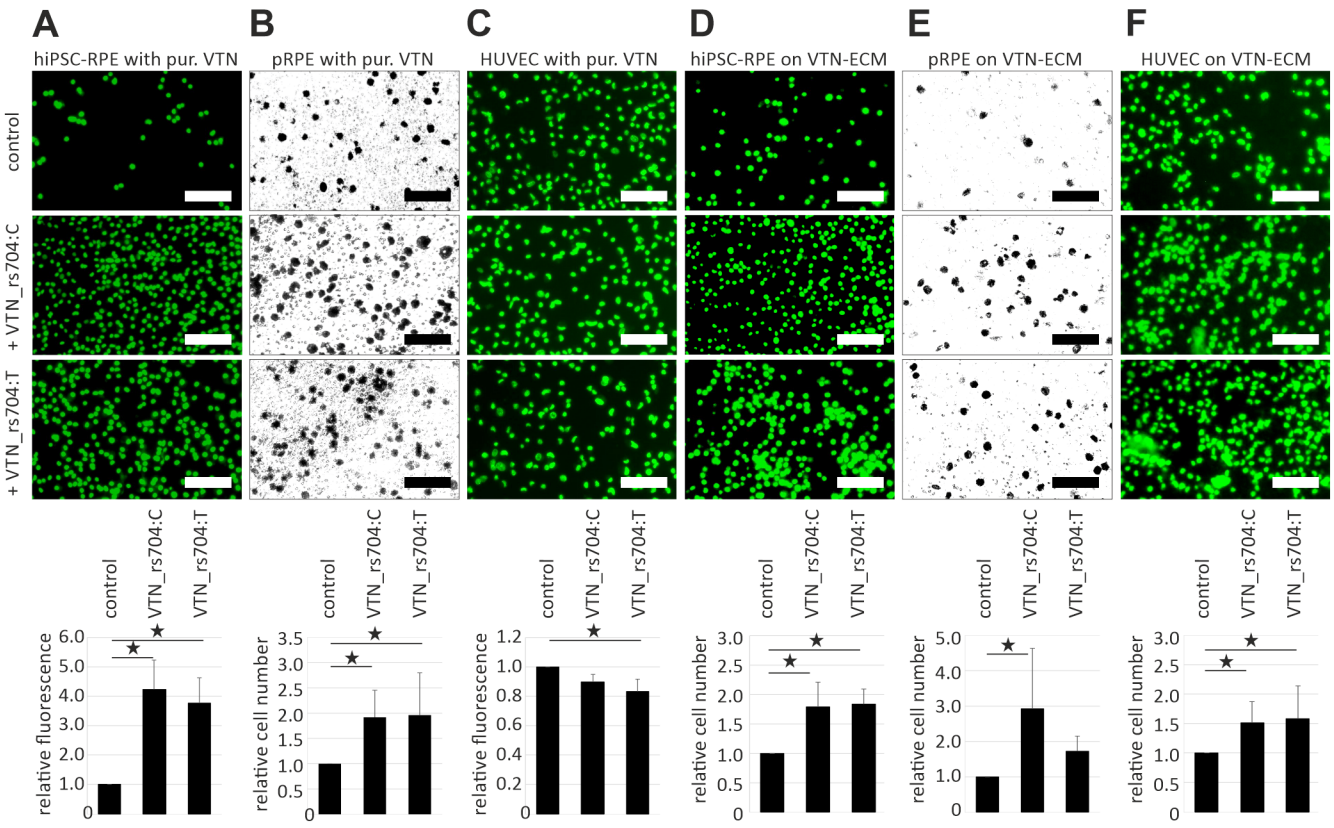

Figure 5. Effect of vitronectin isoforms on RPE and endothelial cell adhesion. (**A**) Suspended hiPSC–RPE cells, (**B**) freshly isolated porcine RPE cells (pRPE), or (**C**) HUVECs were incubated for 24 hours (**A**), 18 hours (**B**), or 20 minutes (**C**) in the presence of purified recombinant VTN_rs704:C, VTN_rs704:T, or control eluate. Subsequently, cell adhesion was determined measuring fluorescence of fluorescently labeled cells in a spectrophotometer (**A**, **C**) or counting cells from 4× micrographs (**B**) using ImageJ. (**D**) Suspended hiPSC–RPE cells, (**E**) freshly isolated pRPE, or (**F**) HUVECs were incubated for 40 minutes (**D**, **E**) or 5 minutes (**F**) on VTN_rs704:C- or VTN_rs704:T-containing ECM or on control ECM. Subsequently, adherent cells were determined by counting cells (fluorescently labeled in **D** and **F**) from 4× micrographs with ImageJ. Data represent mean ± SD of seven (**A**), four (**B**, **E**), or five (**C**, **D**, **F**) independent replicates, calibrated against the control. Asterisks indicate statistically significant differences ($^*P < 0.05$, Kruskal–Wallis test, followed by Dunn's multiple comparison test and Bonferroni correction). Micrographs shown in the figure were taken at 10× magnification (standard, 200 µm).

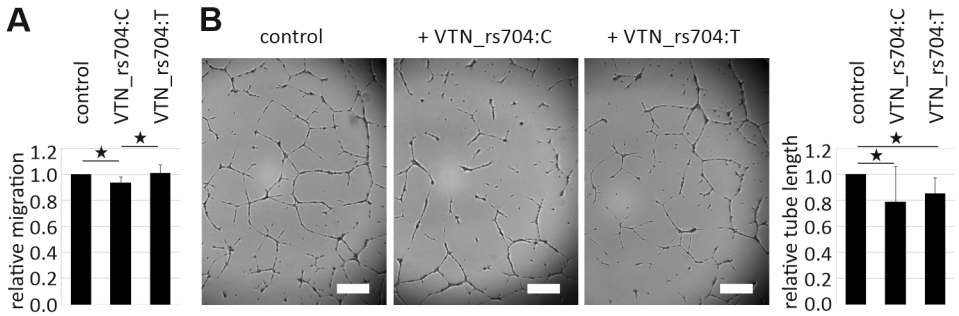

Figure 6. Effect of vitronectin isoforms on HUVEC migration and tube formation. (**A**) To investigate an effect of vitronectin isoforms on endothelial migration, a scratch assay was performed with HUVECs cultivated in the presence of VTN_rs704:C, VTN_rs704:T, or control eluate (see Supplementary Fig. S5), and cell migration was defined as the percentage area closed after 14 hours of incubation. Data represent mean ± SD of six independent replicates, calibrated against the control. (**B**) HUVECs were cultivated in the presence of recombinant VTN_rs704:C, VTN_rs704:T, or control eluate. After 16 hours, the formation of tubular-like structures was followed microscopically (standard, 400 µm). The length of tubular-like structures was measured using ImageJ. Data represent mean ± SD of 11 independent replicates calibrated against the control. Asterisks indicate statistically significant differences ($^*P < 0.05$, Kruskal–Wallis test, followed by Dunn's multiple comparison test and Bonferroni correction).

sion Project (https://gtexportal.org). Bioinformatic analyses including genotype and gene expression data from 49 (non-retinal) tissues revealed no differential effect of the rs704 polymorphism on vitronectin mRNA expression, thus excluding rs704 as an expression quantitative trait locus for *VTN* in the 49 tissues analyzed. However, heterologous expression of the different vitronectin isoforms shows an impact of rs704 on vitronectin protein expression. This is

in agreement with data from a genotype-protein association analysis in human plasma samples from 3301 individuals.[52] In that study, an increase in vitronectin serum levels was associated with AMD-risk variant rs704, classifying rs704 as a protein quantitative trait locus.[52] Increased expression of VTN_rs704:T might be a consequence of different codon usage, which can influence translation kinetics.[53,54] The methionine encoding triplet codon AUG (adenine–uracil–guanine; 22.3 in 1000, found in the risk allele) has a higher frequency than the threonine encoding triplet codon ACG (adenine–cytosine–guanine; 6.2 in 1000).[55] Moreover, rs704:C>T induces an exchange from a polar (threonine) to an unpolar amino acid (methionine). Alterations in translation rate or amino acid composition can affect protein folding and translocation into the endoplasmic reticulum or the Golgi apparatus (summarized in Lodish[56] and Hurtley and Helenius[57]).

As observed before,[26,58,59] rs704 decreases cleavage of full-length vitronectin to a disulfide bond cross-linked form comprised of the 65- and 10-kDa subunits. Studies on functional differences between the cleaved and non-cleaved vitronectin or between VTN_rs704:C and VTN_rs704:T are rare and report controversial results.[59–61] Although Gibson and colleagues[60] failed to detect differences between non-cleaved and cleaved vitronectin in binding to heparin and plasminogen activator inhibitor-1 (PAI-1), Chain and colleagues[59] reported a distinct conformational change after vitronectin cleavage that "buried" a phosphorylation site at amino acid position 378, thus impairing vitronectin phosphorylation. Hazawa and colleagues[61] found that PAI-1 similarly inhibited cleavage of VTN_rs704:C and VTN_rs704:T, and only the non-cleaved but not the cleaved vitronectin protected endothelial cells against radiation-induced cell death.

Our study demonstrated an effect of rs704 on cell binding of vitronectin, which can interact with a variety of molecules on cell surfaces, including integrin receptors,[62–64] urokinase receptor,[65,66] heparin,[67,68] or lipids.[69] Upon interaction with a binding partner, vitronectin changes its structural and functional capacities (reviewed in Preissner and Reuning[50]). The decreased cell surface binding of the AMD-risk-associated vitronectin isoform (VTN_rs704:T) could consequently affect its functionality on various cellular, vitronectin-regulated processes.

Vitronectin is a key constituent of the ECM. In contrast to classical ECM proteins such as collagen, fibronectin, or laminin, which have structural functions, vitronectin is thought to operate as a "matricellular" protein, acting in particular as a modulator of the cell–ECM interface and exerting regulatory functions in a variety of cellular processes such as cell adhesion, angiogenesis, and matrix remodeling (reviewed in Leavesley et al.,[3] Preissner and Reuning,[50] and Schvartz et al.[70]). ECM produced by ARPE-19 cells is composed of characteristic Bruch's membrane proteins[38,39] and supports primary RPE cells to acquire and maintain the RPE phenotype.[38] Therefore, despite the limitation of ARPE-19 cells for studying certain aspects of RPE function due to low polarization, pigmentation, and transepithelial resistance,[71–73] they frequently serve as a model system to recreate Bruch's membrane pathology in culture[12,38,39,74,75] (reviewed in Fields et al.[76]). In our study, heterologous expression of vitronectin by ARPE-19 cells increased deposition and clustering of ECM constituents such as fibronectin, elastin, and collagen VI. This could be a consequence of the matricellular activity of vitronectin. Several studies have shown that vitronectin binds collagen.[77–79] Higher amounts of deposited vitronectin can thus bind higher amounts of collagen, consequently enhancing collagen accumulation at the site of vitronectin deposition, as observed in our analysis. Collagen, on the other hand, interacts with fibronectin and stimulates the formation of a stable fibronectin meshwork.[80–82] Alternatively, vitronectin may directly affect fibronectin deposition; a study by Pankov and colleagues[83] observed that binding of vitronectin to its integrin receptor on the cell surface initiated the assembly of fibronectin, eventually leading to fibronectin fibrillogenesis. Fibronectin in turn can bind elastin[84] and promote elastin deposition.[85] Interestingly, the AMD-risk-associated isoform VTN_rs704:T showed increased deposition and larger cluster size than the non-AMD-risk-associated VTN_rs704:C, which is consistent with the increased expression of VTN_rs704:T observed in our study and in Sun et al.[52] VTN_rs704:T also exerted stronger effects on levels and clustering of fibronectin, elastin, and collagen VI when compared to VTN_rs704:C. A follow-up in-depth characterization of ECM structure (including scanning and transmission electron microscopy) and ECM composition, as well as its consequences on RPE homeostasis, is in progress. Despite the artificial in vitro system, results reproducibly show differences of the two vitronectin isoforms in their ECM deposition and in their effect on other ECM components. The observed functional difference between the two isoforms might also affect ECM deposition in vivo and thus contribute to AMD pathology. AMD eyes characteristically reveal alterations in ECM integrity, specifically the emergence of basal laminar deposits,[86–89] which may cause an impaired diffusion of waste products and nutrients through the RPE (reviewed in Birch and Liang[90] and Bird[91]). Subsequent RPE stress might result in increased RPE death and growth factor production, all characteristic processes in geographic atrophy or choroidal neovascularization (reviewed in Somasundaran et al.[89] and Al-Zamil and Yassin[92]). Moreover, vitronectin is a major component of drusen.[4–6] Increased deposition of risk-associated VTN_rs704:T and concurrent clustering of ECM components such as fibronectin, elastin, and collagen VI could thus be related to the formation of abnormal deposits in Bruch's membrane, hence contributing to AMD development.

Vitronectin plays a key role in the adhesion of cells to the ECM.[93,94] Consistent with this, the addition of recombinant vitronectin or vitronectin-containing ECM strongly increased adhesion of porcine and hiPSC-derived RPE cells. Vitronectin-containing ECM also enhanced adhesion of HUVECs, whereas recombinant vitronectin exerted a different effect: In the latter experiment, vitronectin had no adhesive properties, and the risk-associated isoform VTN_rs704:T even showed a very slight, anti-adhesive effect on HUVECs. This could be the result of a competition of integrin/urokinase receptors and PAI-1 for binding to vitronectin. HUVECs express high amounts of PAI-1,[95–97] which is known to block integrin or urokinase receptor-mediated adhesion due to a close proximity of their respective binding sites on vitronectin.[98–105] Increased attachment of HUVECs to vitronectin-containing ECM could in turn be mediated by other ECM components such as collagen VI or fibronectin, which also exhibited increased deposition in these ECMs.

Interestingly, the two vitronectin isoforms revealed similar effects on cell adhesion, but their capacity to bind to cell surfaces significantly differed. This apparent discrep-

ancy could be explained by the fact that our cell-binding assays show the physical interaction between vitronectin and cells, which can be mediated by a variety of cell surface molecules, such as lipids, different receptors, or heparin.[62–69] In contrast, adhesion is a cellular process that involves the formation of specific multiprotein complexes built by cell adhesion molecules or receptors, ECM proteins, and cytoplasmic plaque or peripheral membrane proteins.[106]

It has been commonly reported that binding of vitronectin to integrin receptors stimulates angiogenic activity in cells.[107–110] However, in our experiments, non-AMD-risk-associated VTN_rs704:C slightly reduced migration compared with control or VTN_rs704:T. Moreover, both isoforms inhibited tube formation by HUVECs. This again could be partially explained by the above-discussed antagonistic effect of PAI-1.[98–105] Several studies have reported an inhibition of cell migration[105,111–113] and tube formation[112,114] by PAI-1, due to blocking integrin or urokinase receptor binding to vitronectin. Furthermore, Yi and colleagues[115] reported that the presence of vitronectin sustains the antiangiogenic activity of several ECM or blood proteins, such as osteonectin, or angiostatin, thus ascribing an indirect antiangiogenic function to vitronectin. Notably, non-AMD-risk-associated VTN_rs704:C showed a stronger impairment of migration and tube formation than AMD-risk-associated VTN_rs704:T, which suggests that the two vitronectin isoforms may exert different regulatory effects on angiogenesis and consequently on choroidal neovascularization.

Of note, there are limitations of this study. Due to the main localization of extracellular vitronectin protein in sub-RPE regions, in specific in Bruch's membrane and the retinal vasculature,[14] our experiments were designed to address the sub-RPE aspects of AMD pathology, and the results should not be extrapolated to the subretinal aspects without further research. Moreover, due to the complex and multifactorial nature of AMD, a variety of other cellular processes may contribute to disease development, e.g. lipid metabolism, complement activation, or oxidative stress responses (reviewed in Datta et al.[116] and Mitchell et al.[117]). The multifaceted character of vitronectin (reviewed in Leavesley et al.,[3] Preissner and Reuning,[50] and Schvartz et al.[70])—for example, as a complement inhibitor[118] or as a putative ligand of the apical RPE-localized integrin receptor which facilitates neural retinal adhesion[119]—might allow its involvement in all of these processes. Additional investigations on functional consequences of rs704 in these pathways and especially subretinal disease aspects are thus required to completely resolve the contribution of vitronectin to AMD pathogenesis. Moreover, to address consequences of the rs704-associated amino acid exchange on structural and functional properties of vitronectin, we applied in vitro studies using recombinant vitronectin. This system benefits from high reproducibility and low background (e.g., without the impact of different genetic backgrounds or growth factors with similar functions), enabling the detection of even small alterations between the different vitronectin isoforms. The in vivo situation in the retina, a highly specified, multilayered tissue of different cell types affected by nutrient supply, growth factors, external and internal stressors, and many additional physiological factors, is surely more complex, requiring caution in the interpretation of the data obtained. Vitronectin functionality (and putative differences between the two isoforms) might be affected or compensated by other matricellular proteins, growth factors, or cytokines. Interestingly, despite the involvement of vitronectin in a variety of essential processes such as wound healing, tissue reorganization, angiogenesis, or matrix remodeling (reviewed in Leavesley et al.[3]), vitronectin-deficient mice show normal development[120] but disturbances in their reaction to tissue injury.[121] It was concluded that vitronectin is not required for normal development but plays a role in the early events of thrombogenesis and tissue repair[121] (reviewed in Leavesley et al.[3]). Connecting these findings to AMD pathogenesis, vitronectin may not exert a major role in retinal integrity until the emergence of disturbances in retinal homeostasis caused by age-related changes, such as accumulation of metabolic debris by RPE cells and Bruch's membrane, neuronal cell loss and degeneration, or alterations in the ocular blood flow.[122,123]

Taken together, this study reveals effects of the AMD-risk-associated rs704 polymorphism on the expression, processing, and functionality of vitronectin, including its capacity to regulate AMD-related processes. This may point to an involvement of rs704 and vitronectin in AMD pathogenesis. Nonetheless, the data do not exclude (additional) pathogenic effects of other variants of the associated genetic locus requiring further scrutiny to consider functional aspects of all genes and variants involved at this locus.

Acknowledgments

The authors thank Martina Esser and Lisa Parakenings (Institute of Human Genetics, University of Regensburg, Germany) for their excellent technical assistance. We thank Christina Kiel (Institute of Human Genetics, University of Regensburg, Germany) for providing the ImageJ script for automated quantification of HUVEC migration. We finally thank reviewer 1 for the intensive discussion on clinical pathology of AMD, specifically on the subretinal processes of the disease pathology. The reviewer's comments and suggestions were excellent and will lead to a follow-up study by us with a focus on subretinal disease processes.

Supported by a scholarship from the Pro Retina Foundation, Aachen, Germany.

Disclosure: **F. Biasella**, None; **K. Plössl**, None; **C. Karl**, None; **B.H.F. Weber**, None; **U. Friedrich**, None

References

1. Smith W, Assink J, Klein R, et al. Risk factors for age-related macular degeneration: pooled findings from three continents. *Ophthalmology*. 2001;108(4):697–704.
2. Chakravarthy U, Evans J, Rosenfeld PJ. Age related macular degeneration. *BMJ*. 2010;340:c981.
3. Leavesley DI, Kashyap AS, Croll T, et al. Vitronectin-master controller or micromanager? *IUBMB Life*. 2013;65(10):807–818.
4. Hageman GS, Mullins RF, Russell SR, Johnson LV, Anderson DH. Vitronectin is a constituent of ocular drusen and the vitronectin gene is expressed in human retinal pigmented epithelial cells. *FASEB J*. 1999;13(3):477–484.
5. Wang L, Clark ME, Crossman DK, et al. Abundant lipid and protein components of drusen. *PLoS One*. 2010;5(4):e10329.
6. Sohn EH, Wang K, Thompson S, et al. Comparison of drusen and modifying genes in autosomal dominant radial drusen and age-related macular degeneration. *Retina*. 2015;35(1):48–57.

7. Russell SR, Mullins RF, Schneider BL, Hageman GS. Location, substructure, and composition of basal laminar drusen compared with drusen associated with aging and age-related macular degeneration. *Am J Ophthalmol*. 2000;129(2):205–214.
8. Curcio CA. Soft drusen in age-related macular degeneration: biology and targeting via the oil spill strategies. *Invest Ophthalmol Vis Sci*. 2018;59(4):AMD160–AMD181.
9. Rudolf M, Malek G, Messinger JD, Clark ME, Wang L, Curcio CA. Sub-retinal drusenoid deposits in human retina: organization and composition. *Exp Eye Res*. 2008;87(5):402–408.
10. Spaide RF, Ooto S, Curcio CA. Subretinal drusenoid deposits AKA pseudodrusen. *Surv Ophthalmol*. 2018;63(6):782–815.
11. Johnson LV, Leitner WP, Staples MK, Anderson DH. Complement activation and inflammatory processes in Drusen formation and age related macular degeneration. *Exp Eye Res*. 2001;73(6):887–896.
12. Gong J, Cai H, Noggle S, et al. Stem cell-derived retinal pigment epithelium from patients with age-related macular degeneration exhibit reduced metabolism and matrix interactions. *Stem Cells Transl Med*. 2020;9(3):364–376.
13. Wasmuth S, Lueck K, Baehler H, Lommatzsch A, Pauleikhoff D. Increased vitronectin production by complement-stimulated human retinal pigment epithelial cells. *Invest Ophthalmol Vis Sci*. 2009;50(11):5304–5309.
14. Anderson DH, Hageman GS, Mullins RF, et al. Vitronectin gene expression in the adult human retina. *Invest Ophthalmol Vis Sci*. 1999;40(13):3305–3315.
15. Li M, Jia C, Kazmierkiewicz KL, et al. Comprehensive analysis of gene expression in human retina and supporting tissues. *Hum Mol Genet*. 2014;23(15):4001–4014.
16. Curcio CA, Johnson M. Structure, Function, and Pathology of Bruch's Membrane. In Ryan SJ, Sadda SR, Hinton DR , et al., eds. *Retina*. 5th ed., Vol. 1. Philadelphia, PA: Saunders; 2012:465–481.
17. Dejana E, Conforti G, Zanetti A, Lampugnani MG, Marchisio PC. Receptors for extracellular matrix proteins in endothelial cells. In: Catravas J , ed. *Vascular Endothelium: Receptors and Transduction Mechanisms*. Boston, MA: Springer; 1989:141–147.
18. Preissner KT, Seiffert D. Role of vitronectin and its receptors in haemostasis and vascular remodeling. *Thromb Res*. 1998;89(1):1–21.
19. Stockmann A, Hess S, Declerck P, Timpl R, Preissner KT. Multimeric vitronectin. Identification and characterization of conformation-dependent self-association of the adhesive protein. *J Biol Chem*. 1993;268(30):22874–22882.
20. Seiffert D. Constitutive and regulated expression of vitronectin. *Histol Histopathol*. 1997;12(3):787–797.
21. Fritsche LG, Igl W, Bailey JN, et al. A large genome-wide association study of age-related macular degeneration highlights contributions of rare and common variants. *Nat Genet*. 2016;48(2):134–143.
22. Sveinbjornsson G, Albrechtsen A, Zink F, et al. Weighting sequence variants based on their annotation increases power of whole-genome association studies. *Nat Genet*. 2016;48(3):314–317.
23. Pal LR, Yu CH, Mount SM, Moult J. Insights from GWAS: emerging landscape of mechanisms underlying complex trait disease. *BMC Genomics*. 2015;16(suppl 8):S4.
24. Kleinman ME, Ambati J. Molecular mechanisms of neovascularization in AMD. *Retinal Physician*. 2009; http://www.retinalphysician.com/article.aspx?article=101897.
25. Campochiaro PA. Molecular pathogenesis of retinal and choroidal vascular diseases. *Prog Retin Eye Res*. 2015;49:67–81.
26. Tollefsen DM, Weigel CJ, Kabeer MH. The presence of methionine or threonine at position 381 in vitronectin is correlated with proteolytic cleavage at arginine 379. *Biol Chem*. 1990;265(17):9778–9781.
27. Nachtigal AL, Milenkovic A, Brandl C, et al. Mutation-dependent pathomechanisms determine the phenotype in the bestrophinopathies. *Int J Mol Sci*. 2020;21(5):1597.
28. Okita K, Yamakawa T, Matsumura Y, et al. An efficient nonviral method to generate integration-free human-induced pluripotent stem cells from cord blood and peripheral blood cells. *Stem Cells*. 2013;31(3):458–466.
29. Brandl C, Zimmermann SJ, Milenkovic VM, et al. In-depth characterisation of retinal pigment epithelium (RPE) cells derived from human induced pluripotent stem cells (hiPSC). *Neuromolecular Med*. 2014;16(3):551–564.
30. Friedrich U, Stohr H, Hilfinger D, et al. The Na/K-ATPase is obligatory for membrane anchorage of retinoschisin, the protein involved in the pathogenesis of X-linked juvenile retinoschisis. *Hum Mol Genet*. 2011;20(6):1132–1142.
31. Friedrich U, Myers CA, Fritsche LG, et al. Risk- and non-risk-associated variants at the 10q26 AMD locus influence ARMS2 mRNA expression but exclude pathogenic effects due to protein deficiency. *Hum Mol Genet*. 2011;20(7):1387–1399.
32. Sambrook J, Russell DW. Calcium-phosphate-mediated transfection of eukaryotic cells with plasmid DNAs. *Cold Spring Harb Protoc*. 2006;2006(1):pdb.prot3871.
33. Plössl K, Royer M, Bernklau S, et al. Retinoschisin is linked to retinal Na/K-ATPase signaling and localization. *Mol Biol Cell*. 2017;28(16):2178–2189.
34. Plössl K, Weber BH, Friedrich U. The X-linked juvenile retinoschisis protein retinoschisin is a novel regulator of mitogen-activated protein kinase signalling and apoptosis in the retina. *J Cell Mol Med*. 2017;21(4):768–780.
35. Laemmli UK. Cleavage of structural proteins during the assembly of the head of bacteriophage T4. *Nature*. 1970;227(5259):680–685.
36. Plössl K, Straub K, Schmid V, et al. Identification of the retinoschisin-binding site on the retinal Na/K-ATPase. *PLoS One*. 2019;14(5):e0216320.
37. Gómez NM, Tamm ER, Strauβ O. Role of bestrophin-1 in store-operated calcium entry in retinal pigment epithelium. *Pflügers Arch*. 2013;465(4):481–495.
38. McLenachan S, Hao E, Zhang D, Zhang L, Edel M, Chen F. Bioengineered Bruch's-like extracellular matrix promotes retinal pigment epithelial differentiation. *Biochem Biophys Rep*. 2017;10:178–185.
39. Fernandez-Godino R, Bujakowska KM, Pierce EA. Changes in extracellular matrix cause RPE cells to make basal deposits and activate the alternative complement pathway. *Hum Mol Genet*. 2018;27(1):147–159.
40. Schmid V, Plossl K, Schmid C, Bernklau S, Weber BHF, Friedrich U. Retinoschisin and cardiac glycoside crosstalk at the retinal Na/K-ATPase. *Invest Ophthalmol Vis Sci*. 2020;61(5):1.
41. Ponce ML. Tube formation: an in vitro matrigel angiogenesis assay. *Methods Mol Biol*. 2009;467:183–188.
42. Carpentier G. Angiogenesis analyzer for ImageJ, Available at: http://image.bio.methods.free.fr/ImageJ/?Angiogenesis-Analyzer-for-ImageJ&lang. Accessed November 16, 2020.
43. Liang CC, Park AY, Guan JL. In vitro scratch assay: a convenient and inexpensive method for analysis of cell migration in vitro. *Nat Protoc*. 2007;2(2):329–333.
44. Forest DL, Johnson LV, Clegg DO. Cellular models and therapies for age-related macular degeneration. *Dis Model Mech*. 2015;8(5):421–427.

Investigative Ophthalmology & Visual Science

45. Shin TM, Isas JM, Hsieh CL, et al. Formation of soluble amyloid oligomers and amyloid fibrils by the multifunctional protein vitronectin. *Mol Neurodegener*. 2008;3:16.
46. Chillakuri CR, Jones C, Mardon HJ. Heparin binding domain in vitronectin is required for oligomerization and thus enhances integrin mediated cell adhesion and spreading. *FEBS Lett*. 2010;584(15):3287–3291.
47. Wang T, Zhou A, Waters CT, O'Connor E, Read RJ, Trump D. Molecular pathology of X linked retinoschisis: mutations interfere with retinoschisin secretion and oligomerisation. *Br J Ophthalmol*. 2006;90(1):81–86.
48. Wu WW, Molday RS. Defective discoidin domain structure, subunit assembly, and endoplasmic reticulum processing of retinoschisin are primary mechanisms responsible for X-linked retinoschisis. *Biol Chem*. 2003;278(30):28139–28146.
49. Plössl K, Schmid V, Straub K, et al. Pathomechanism of mutated and secreted retinoschisin in X-linked juvenile retinoschisis. *Exp Eye Res*. 2018;177:23–34.
50. Preissner KT, Reuning U. Vitronectin in vascular context: facets of a multitalented matricellular protein. *Semin Thromb Hemost*. 2011;37(4):408–424.
51. Shirinifard A, Glazier JA, Swat M, et al. Adhesion failures determine the pattern of choroidal neovascularization in the eye: a computer simulation study. *PLoS Comput Biol*. 2012;8(5):e1002440.
52. Sun BB, Maranville JC, Peters JE, et al. Genomic atlas of the human plasma proteome. *Nature*. 2018;558(7708):73–79.
53. Cannarozzi G, Schraudolph NN, Faty M, et al. A role for codon order in translation dynamics. *Cell*. 2010;141(2):355–367.
54. Tuller T, Waldman YY, Kupiec M, Ruppin E. Translation efficiency is determined by both codon bias and folding energy. *Proc Natl Acad Sci USA*. 2010;107(8):3645–3650.
55. Benson DA, Karsch-Mizrachi I, Lipman DJ, Ostell J, Wheeler DL. GenBank. *Nucleic Acids Res*. 2005;33(Database issue):D34–D38.
56. Lodish HF. Transport of secretory and membrane glycoproteins from the rough endoplasmic reticulum to the Golgi. A rate-limiting step in protein maturation and secretion. *J Biol Chem*. 1988;263(5):2107–2110.
57. Hurtley SM, Helenius A. Protein oligomerization in the endoplasmic reticulum. *Annu Rev Cell Biol*. 1989;5:277–307.
58. Chain D, Korc-Grodzicki B, Kreizman T, Shaltiel S. The phosphorylation of the two-chain form of vitronectin by protein kinase A is heparin dependent. *FEBS Lett*. 1990;269(1):221–225.
59. Chain D, Korc-Grodzicki B, Kreizman T, Shaltiel S. Endogenous cleavage of the Arg-379-Ala-380 bond in vitronectin results in a distinct conformational change which 'buries' Ser-378, its site of phosphorylation by protein kinase A. *Biochem J*. 1991;274 (Pt 2):387–394.
60. Gibson AD, Peterson CB. Full-length and truncated forms of vitronectin provide insight into effects of proteolytic processing on function. *Biochim Biophys Acta*. 2001;1545(1–2):289–304.
61. Hazawa M, Yasuda T, Saotome-Nakamura A, et al. Intra- and extracellular plasminogen activator inhibitor-1 regulate effect of vitronectin against radiation-induced endothelial cell death. *Vascul Pharmacol*. 2016;87:150–158.
62. Felding-Habermann B, Cheresh DA. Vitronectin and its receptors. *Curr Opin Cell Biol*. 1993;5(5):864–868.
63. Horton MA. The alpha v beta 3 integrin "vitronectin receptor". *Int J Biochem Cell Biol*. 1997;29(5):721–725.
64. Spreghini E, Gismondi A, Piccoli M, Santoni G. Evidence for alphavbeta3 and alphavbeta5 integrin-like vitronectin (VN) receptors in *Candida albicans* and their involvement in yeast cell adhesion to VN. *J Infect Dis*. 1999;180(1):156–166.
65. Wei Y, Waltz DA, Rao N, Drummond RJ, Rosenberg S, Chapman HA. Identification of the urokinase receptor as an adhesion receptor for vitronectin. *J Biol Chem*. 1994;269(51):32380–32388.
66. Madsen CD, Ferraris GM, Andolfo A, Cunningham O, Sidenius N. uPAR-induced cell adhesion and migration: vitronectin provides the key. *J Cell Biol*. 2007;177(5):927–939.
67. Francois PP, Preissner KT, Herrmann M, et al. Vitronectin interaction with glycosaminoglycans. Kinetics, structural determinants, and role in binding to endothelial cells. *J Biol Chem*. 1999;274(53):37611–37619.
68. Akama T, Yamada KM, Seno N, et al. Immunological characterization of human vitronectin and its binding to glycosaminoglycans. *J Biochem*. 1986;100(5):1343–1351.
69. Yoneda A, Ogawa H, Kojima K, Matsumoto I. Characterization of the ligand binding activities of vitronectin: interaction of vitronectin with lipids and identification of the binding domains for various ligands using recombinant domains. *Biochemistry*. 1998;37(18):6351–6360.
70. Schvartz I, Seger D, Shaltiel S. Vitronectin. *Int J Biochem Cell Biol*. 1999;31(5):539–544.
71. Ablonczy Z, Dahrouj M, Tang PH, et al. Human retinal pigment epithelium cells as functional models for the RPE in vivo. *Invest Ophthalmol Vis Sci*. 2011;52(12):8614–8620.
72. Luo Y, Zhuo Y, Fukuhara M, Rizzolo LJ. Effects of culture conditions on heterogeneity and the apical junctional complex of the ARPE-19 cell line. *Invest Ophthalmol Vis Sci*. 2006;47(8):3644–3655.
73. Samuel W, Jaworski C, Postnikova OA, et al. Appropriately differentiated ARPE-19 cells regain phenotype and gene expression profiles similar to those of native RPE cells. *Mol Vis*. 2017;23:60–89.
74. Moreira EF, Cai H, Tezel TH, Fields MA, Del Priore LV. Reengineering human Bruch's membrane increases rod outer segment phagocytosis by human retinal pigment epithelium. *Transl Vis Sci Technol*. 2015;4(5):10.
75. Corydon TJ, Mann V, Slumstrup L, et al. Reduced expression of cytoskeletal and extracellular matrix genes in human adult retinal pigment epithelium cells exposed to simulated microgravity. *Cell Physiol Biochem*. 2016;40(1–2):1–17.
76. Fields MA, Del Priore LV, Adelman RA, Rizzolo LJ. Interactions of the choroid, Bruch's membrane, retinal pigment epithelium, and neurosensory retina collaborate to form the outer blood-retinal-barrier. *Prog Retin Eye Res*. 2020;76:100803.
77. Gebb C, Hayman EG, Engvall E, Ruoslahti E. Interaction of vitronectin with collagen. *J Biol Chem*. 1986;261(35):16698–16703.
78. Sano K, Asanuma-Date K, Arisaka F, Hattori S, Ogawa H. Changes in glycosylation of vitronectin modulate multimerization and collagen binding during liver regeneration. *Glycobiology*. 2007;17(7):784–794.
79. Date K, Suzuki R, Oda-Tamai S, Ogawa H. Vitronectins produced by human cirrhotic liver and CCl_4-treated rats differ in their glycosylation pattern and tissue remodeling activity. *FEBS Open Bio*. 2019;9(4):755–768.
80. Sabatelli P, Bonaldo P, Lattanzi G, et al. Collagen VI deficiency affects the organization of fibronectin in the extracellular matrix of cultured fibroblasts. *Matrix Biol*. 2001;20(7):475–486.
81. Katagiri Y, Brew SA, Ingham KC. All six modules of the gelatin-binding domain of fibronectin are required for full affinity. *J Biol Chem*. 2003;278(14):11897–11902.

Investigative Ophthalmology & Visual Science

82. Vakonakis I, Staunton D, Ellis IR, et al. Motogenic sites in human fibronectin are masked by long range interactions. *J Biol Chem*. 2009;284(23):15668–15675.
83. Pankov R, Cukierman E, Katz BZ, et al. Integrin dynamics and matrix assembly: tensin-dependent translocation of alpha(5)beta(1) integrins promotes early fibronectin fibrillogenesis. *J Cell Biol*. 2000;148(5):1075–1090.
84. Harumiya S, Jung SK, Sakano Y, Fujimoto D. Interaction of human plasma fibronectin with alpha-elastin. *J Biochem*. 1993;113(6):710–714.
85. Pezzoli D, Di Paolo J, Kumra H, et al. Fibronectin promotes elastin deposition, elasticity and mechanical strength in cellularised collagen-based scaffolds. *Biomaterials*. 2018;180:130–142.
86. Green WR, Enger C. Age-related macular degeneration histopathologic studies. The 1992 Lorenz E. Zimmerman Lecture. *Ophthalmology*. 1993;100(10):1519–1535.
87. Sarks JP, Sarks SH, Killingsworth MC. Evolution of soft drusen in age-related macular degeneration. *Eye (Lond)*. 1994;8(Pt 3):269–283.
88. Curcio CA, Millican CL. Basal linear deposit and large drusen are specific for early age-related maculopathy. *Arch Ophthalmol*. 1999;117(3):329–339.
89. Somasundaran S, Constable IJ, Mellough CB, Carvalho LS. Retinal pigment epithelium and age-related macular degeneration: a review of major disease mechanisms [published online ahead of print July 24, 2020]. *J Clin Exp Ophthalmol*, https://doi.org/10.1111/ceo.13834.
90. Birch DG, Liang FQ. Age-related macular degeneration: a target for nanotechnology derived medicines. *Int J Nanomedicine*. 2007;2(1):65–77.
91. Bird A. Role of retinal pigment epithelium in age-related macular disease: a systematic review [published online ahead of print September 19, 2020]. *Br J Ophthalmol*, https://doi.org/10.1136/bjophthalmol-2020-317447.
92. Al-Zamil WM, Yassin SA. Recent developments in age-related macular degeneration: a review. *Clin Interv Aging*. 2017;12:1313–1330.
93. Tomasini BR, Mosher DF. Vitronectin. *Prog Hemost Thromb*. 1991;10:269–305.
94. Preissner KT. Structure and biological role of vitronectin. *Annu Rev Cell Biol*. 1991;7:275–310.
95. Daniel AE, Timmerman I, Kovacevic I, et al. Plasminogen activator inhibitor-1 controls vascular integrity by regulating VE-cadherin trafficking. *PLoS One*. 2015;10(12):e0145684.
96. Bartha K, Declerck PJ, Moreau H, Nelles L, Collen D. Synthesis and secretion of plasminogen activator inhibitor 1 by human endothelial cells in vitro. Effect of active site mutagenized tissue-type plasminogen activator. *J Biol Chem*. 1991;266(2):792–797.
97. Konkle BA, Ginsburg D. The addition of endothelial cell growth factor and heparin to human umbilical vein endothelial cell cultures decreases plasminogen activator inhibitor-1 expression. *J Clin Invest*. 1988;82(2):579–585.
98. Declerck PJ, De Mol M, Alessi MC, et al. Purification and characterization of a plasminogen activator inhibitor 1 binding protein from human plasma. Identification as a multimeric form of S protein (vitronectin). *J Biol Chem*. 1988;263(30):15454–15461.
99. Mimuro J, Loskutoff DJ. Purification of a protein from bovine plasma that binds to type 1 plasminogen activator inhibitor and prevents its interaction with extracellular matrix. Evidence that the protein is vitronectin. *J Biol Chem*. 1989;264(2):936–939.
100. Salonen EM, Vaheri A, Pollanen J, et al. Interaction of plasminogen activator inhibitor (PAI-1) with vitronectin. *J Biol Chem*. 1989;264(11):6339–6343.
101. Wun TC, Palmier MO, Siegel NR, Smith CE. Affinity purification of active plasminogen activator inhibitor-1 (PAI-1) using immobilized anhydrourokinase. Demonstration of the binding, stabilization, and activation of PAI-1 by vitronectin. *J Biol Chem*. 1989;264(14):7862–7868.
102. Deng G, Curriden SA, Wang S, Rosenberg S, Loskutoff DJ. Is plasminogen activator inhibitor-1 the molecular switch that governs urokinase receptor-mediated cell adhesion and release? *J Cell Biol*. 1996;134(6):1563–1571.
103. Deng G, Curriden SA, Hu G, Czekay RP, Loskutoff DJ. Plasminogen activator inhibitor-1 regulates cell adhesion by binding to the somatomedin B domain of vitronectin. *J Cell Physiol*. 2001;189(1):23–33.
104. Stefansson S, Su EJ, Ishigami S, et al. The contributions of integrin affinity and integrin-cytoskeletal engagement in endothelial and smooth muscle cell adhesion to vitronectin. *J Biol Chem*. 2007;282(21):15679–15689.
105. Kjoller L, Kanse SM, Kirkegaard T, et al. Plasminogen activator inhibitor-1 represses integrin- and vitronectin-mediated cell migration independently of its function as an inhibitor of plasminogen activation. *Exp Cell Res*. 1997;232(2):420–429.
106. Gumbiner BM. Cell adhesion: the molecular basis of tissue architecture and morphogenesis. *Cell*. 1996;84(3):345–357.
107. Brooks PC, Clark RA, Cheresh DA. Requirement of vascular integrin alpha v beta 3 for angiogenesis. *Science*. 1994;264(5158):569–571.
108. Soldi R, Mitola S, Strasly M, Defilippi P, Tarone G, Bussolino F. Role of alphavbeta3 integrin in the activation of vascular endothelial growth factor receptor-2. *EMBO J*. 1999;18(4):882–892.
109. Brakenhielm E. Substrate matters: reciprocally stimulatory integrin and VEGF signaling in endothelial cells. *Circ Res*. 2007;101(6):536–538.
110. Mahabeleshwar GH, Byzova TV. Angiogenesis in melanoma. *Semin Oncol*. 2007;34(6):555–565.
111. Stefansson S, Lawrence DA. The serpin PAI-1 inhibits cell migration by blocking integrin alpha V beta 3 binding to vitronectin. *Nature*. 1996;383(6599):441–443.
112. Brandal S, Blake CM, Sullenger BA, Fortenberry YM. Effects of plasminogen activator inhibitor-1-specific RNA aptamers on cell adhesion, motility, and tube formation. *Nucleic Acid Ther*. 2011;21(6):373–381.
113. Waltz DA, Natkin LR, Fujita RM, Wei Y, Chapman HA. Plasmin and plasminogen activator inhibitor type 1 promote cellular motility by regulating the interaction between the urokinase receptor and vitronectin. *J Clin Invest*. 1997;100(1):58–67.
114. Isogai C, Laug WE, Shimada H, et al. Plasminogen activator inhibitor-1 promotes angiogenesis by stimulating endothelial cell migration toward fibronectin. *Cancer Res*. 2001;61(14):5587–5594.
115. Yi M, Sakai T, Fassler R, Ruoslahti E. Antiangiogenic proteins require plasma fibronectin or vitronectin for in vivo activity. *Proc Natl Acad Sci USA*. 2003;100(20):11435–11438.
116. Datta S, Cano M, Ebrahimi K, Wang L, Handa JT. The impact of oxidative stress and inflammation on RPE degeneration in non-neovascular AMD. *Prog Retin Eye Res*. 2017;60:201–218.
117. Mitchell P, Liew G, Gopinath B, Wong TY. Age-related macular degeneration. *Lancet*. 2018;392(10153):1147–1159.
118. Milis L, Morris CA, Sheehan MC, Charlesworth JA, Pussell BA. Vitronectin-mediated inhibition of complement: evidence for different binding sites for C5b-7 and C9. *J Clin Exp Immunol*. 1993;92(1):114–119.

Investigative Ophthalmology & Visual Science

119. Nandrot EF, Chang Y, Finnemann SC. Alphavbeta5 integrin receptors at the apical surface of the RPE: one receptor, two functions. *Adv Exp Med Biol*. 2008;613:369–375.
120. Zheng X, Saunders TL, Camper SA, Samuelson LC, Ginsburg D. Vitronectin is not essential for normal mammalian development and fertility. *Proc Natl Acad Sci USA*. 1995;92(26):12426–12430.
121. Jang YC, Tsou R, Gibran NS, Isik FF. Vitronectin deficiency is associated with increased wound fibrinolysis and decreased microvascular angiogenesis in mice. *Surgery*. 2000;127(6):696–704.
122. Ehrlich R, Harris A, Kheradiya NS, Winston DM, Ciulla TA, Wirostko B. Age-related macular degeneration and the aging eye. *Clin Interv Aging*. 2008;3(3):473–482.
123. Salvi SM, Akhtar S, Currie Z. Ageing changes in the eye. *Postgrad Med J*. 2006;82(971):581–587.

Investigative Ophthalmology & Visual Science